


Enoxacin Exerts Anti-Tumor Effects Against Prostate Cancer Through Inducing Apoptosis

Technology in Cancer Research & Treatment
Volume 20: 1-8
© The Author(s) 2021
Article reuse guidelines:
sagepub.com/journals-permissions
DOI: 10.1177/1533033821995284
journals.sagepub.com/home/tct


Hongyan Xu, BS¹ , Minghuan Mao, PhD¹, Rui Zhao, MS², and Qing Zhao, BS¹

Abstract

Background: Prostate cancer is the most commonly diagnosed cancer and second leading cause of cancer death in men. Enoxacin, a third-generation fluoroquinolone antibiotic, was found with anti-proliferative effects against many cancer types. This study was to further investigate its effects against prostate cancer and explore the underlying molecular mechanisms. **Methods:** PC-3 cells were treated with Enoxacin at different concentrations. Tumor model was established by subcutaneously injecting PC-3 cells into nude mice. MTT assay was used to detect cell viability. ELISA assay, Annexin V/PI staining and TUNEL assay were used to detect apoptosis. RT-qPCR and western blot were used to detect the gene and protein expression, respectively. **Results:** Our data showed that Enoxacin inhibited PC-3 cell proliferation and induced the apoptosis through up-regulating the expression of pro-apoptotic proteins, while down-regulating expression levels of anti-apoptotic proteins. Moreover, Enoxacin increased the gene and protein expression of the autophagy and endoplasmic reticulum stress markers. Treating tumor-bearing mice with Enoxacin significantly inhibited tumor growth in xenograft tumor model. **Conclusion:** Our results suggested that Enoxacin could be developed as a potential anti-tumor agent against prostate carcinoma.

Keywords

enoxacin, prostate cancer, apoptosis, autophagy, endoplasmic reticulum stress

Received: July 12, 2020; Revised: January 03, 2021; Accepted: January 25, 2021.

Background

Prostate cancer is the most commonly diagnosed non-cutaneous malignancy and the second leading cause of cancer-related death in men in developed countries.¹ Androgen deprivation therapy (ADT) is the standard of care for prostate cancer, owing to the essential role of the androgen receptor (AR) in the normal growth and development of the prostate gland, as well as in prostate carcinogenesis.² Although ADT offers near certain remissions lasting 1-2 years in most patients, cancer cells become resistant with the emergence of castration-resistant prostate cancer (CRPC). Docetaxel, a chemotherapeutic inhibitor of microtubule depolymerization, offered a modest 2.5 months median prolongation in overall survival for CRPC patients. However, acquired resistance to the drug eventually emerges.^{3,4} Thereafter, it is definitely imperative to search for novel therapeutic agents with new mode of action.

Apoptosis is a precisely self-regulating death process and plays a crucial role in controlling development and homeostasis

of multicellular organisms. Its malfunction has been closely associated with various diseases, including cancers.⁵ As a major apoptotic route for apoptosis, the intrinsic mitochondrial pathway plays a central role in regulating apoptotic processes in various cancer cells.⁶ Studies showed that active endoplasmic reticulum (ER) stress was related to the intrinsic mitochondrial apoptosis pathway through 3 sensors: GRP78, IRE1, and ATF6.^{7,8} Once these sensors are released from Bip,

¹ Second Department of Urology, the Fourth Affiliated Hospital of China Medical University, Shenyang City, Liaoning Province, China

² Fourth Clinical College of China Medical University, Shenyang City, Liaoning Province, China

Corresponding Author:

Hongyan Xu, BS, Second Department of Urology, the Fourth Affiliated Hospital of China Medical University, No. 4 Chongshan East Road, Huanggu District, Shenyang City, Liaoning Province 110032, China.
Email: xhyhongyan12@163.com



downstream effectors are activated to trigger pro-apoptotic signals through targeting on several apoptotic genes.⁹

As a third-generation fluoroquinolone antibiotic, Enoxacin inhibited tumor cell proliferation in many cancer types.¹⁰⁻¹² In this study, its effects were further investigated against prostate carcinoma. Our results demonstrated Enoxacin exhibited potent anti-tumor activities, as evidenced by inhibiting the proliferation and slowing tumor growth of prostate carcinoma, providing rationale to develop Enoxacin as a new potential therapeutic agent against prostate cancer.

Materials and Methods

Cell lines, Reagents and Chemicals

Normal human prostate/stroma cell line WPMY-1, lung adenocarcinoma cell line A549, pancreatic adenocarcinoma cell line PANC-1, hepatocellular carcinoma cell line HepG2, prostate adenocarcinoma cell line PC-3, prostate carcinoma cell lines DU145, LNCaP and C4-2, glioblastoma cell line U251, squamous cell carcinoma cell line SK-MES-1, breast adenocarcinoma cell line MCF-7, and osteosarcoma cell line MG-63 were purchased from Shanghai Cell Bank (Shanghai, China). Roswell Park Memorial Institute (RPMI) 1640 medium and fetal bovine serum (FBS) were purchased from Gibco (Gaithersburg, USA). 3,3'-dihexyloxycarbocyanine iodide (DiOC₆) was purchased from Sigma (St. Louis, MO, USA). Caspase-3/9 colorimetric assay kits and cytochrome-c immunoassay kit were purchased from R&D Systems (Minneapolis, MN, USA). 5,5',6,6'-tetrachloro-1,1',3,3'-tetraethylbenzimidazolylcarbocyanine iodide (JC-1) was purchased from Molecular Probes (CA, USA). Annexin V/PI apoptosis assay kit was purchased from GeneCopoeia (Rockville, MD, USA). PCR reagents were purchased from Thermo Fisher (Waltham, MA, USA). Taxol and Enoxacin were purchased from Sigma (St. Louis, MO, USA). All solvents were purchased from Sino-pharm Co. Ltd. (Shanghai, China). Enoxacin was dissolved in PBS for *in vitro* and *in vivo* experiments.

Mouse

Six-week old male nude mice (Balb/c-nu/nu) were purchased from Vital River Ltd. (Shanghai, China) and maintained in sterile facility with free access to water and food during the whole experiments. The animal procedures were approved by the Institutional Animal Care and Use Committee of xxx with the protocol No. (2018-1133) and performed in strict accordance with the regulation of the Use of Animals.

MTT Assay

Cells were cultured in RPMI1640 medium supplemented with 10% FBS, 100 µg/mL Penicillin/Streptomycin at 37 °C in an atmosphere of 5% CO₂. 2×10^4 cells/well were seeded in 96-well plates and treated with Enoxacin (1-1000 µM) or Taxol (1-1000 nM) for 48 h. Cells treated with DMSO were used as negative control. After washing, cells were incubated

for 4 h with 5 mg/mL of MTT. The formazan crystals were dissolved in DMSO after removing the MTT solution. Absorbance was measured at 570 nm using the 96-well plate reader. Cell viability was expressed as the percentage of the negative control, which was set to 100%.

Cell Proliferation Assay

3×10^5 PC-3 cells/well were seeded in 6-well plates and treated with Enoxacin at 1, 3, 10 µM. PC3 cells treated with DMSO were used as negative control. Cell number was measured at 24, 48 and 72 h by cell counter (Vi-Cell, Beckman Coulter).

Mitochondrial Membrane Potential (MMP) Measurement

MMP was measured by flow cytometry. Briefly, after treatment, PC-3 cells were harvested and re-suspended in 500 µl DiOC₆ for 15 min at 37°C in the dark. After rinsing twice, fluorescence intensity was measured by flow cytometry.

Cytochrome-c Assay

After treatment, PC-3 cells were re-suspended in 1 ml of extraction buffer and homogenized in an ice-cold Dounce tissue grinder (Catalog No. 1998-1, BioVision). The mitochondrial and cytosol subcellular fractions were isolated with Mitochondria/Cytosol Fractionation Kit (Catalog No. K256-100, BioVision) according to the manufacturer's instructions. The cytochrome-c in mitochondrial or cytosol subcellular fractions was measured by the assay kit (Catalog No.: MCTC0, R&D systems) according to the manufacturer's instructions. Then the ratio of cytochrome-c content in the cytosol fraction and in the mitochondria fraction were calculated.

Apoptosis Measurement

After treatment, PC-3 cells were collected and re-suspended in Annexin V binding buffer. Annexin V (5 µl) and propidium iodide (1 µl) were added to each sample. Samples were incubated for 10 min in the dark at room temperature. Apoptotic cells were quantified by flow cytometry (BD Biosciences, San Jose, CA, USA).

Caspase Activity Measurement

After treatment, PC-3 cells were lysed and activities of caspases were determined using caspase-3 and caspase-9 colorimetric assay kits in accordance with the manufacturer's protocols (R&D Systems).

Terminal Deoxynucleotidyl Transferase dUTP Nick End Labeling (TUNEL) Assay

Tumor samples were harvested and fixed with 4% paraformaldehyde for 4 h. After dehydration with graded sucrose solution,

tumor samples were embedded in Optimal Cutting Temperature compound and 10 μm sections were cut sagittally with freezing microtome (Sakura, the Netherlands). Apoptosis was detected by the In Situ Cell Death Detection Kit (Roche Applied Science, IN, USA) in accordance with the manufacturer's protocols. Sections were visualized under the Olympus BX60 microscope (Olympus, Shinjuku, Japan).

Quantitative Real-Time PCR

Total RNA was extracted with the Trizol and mRNA was transcribed into cDNA with SuperScript master mix (Biorad). Quantitative PCR was run on StepOne system using SYBR green Supermix (Thermo Fisher) with comparative Ct value method.

Western Blot Analysis

After treatment, PC-3 cells were harvested and lysed with RIPA buffer (Sigma). Protein concentration was determined using the bicinchoninic acid method. Equal protein (40 μg) was subjected to sodium dodecyl sulfate polyacrylamide gel

electrophoresis with 4-12% gel and then transferred to polyvinylidene difluoride membranes (Millipore, Darmstadt, Germany). Membranes were blocked with 1% bovine serum albumin for 1 h and then incubated with different primary antibodies overnight at 4°C. Membranes were then incubated with the secondary antibody for 1 h. The bands were detected by the enhanced chemiluminescence system.

Xenograft Tumor Model

5×10^6 PC-3 cells were injected subcutaneously into right flank of nude mice. When tumor volume reached 50-100 mm^3 , tumor-bearing mice were divided into 3 groups (5 mice per group) and started the treatment. Enoxacin (1 and 2 mg/kg) was given by intraperitoneal injection 3 times per week, mice treated with PBS as negative control. When tumor volume reached 1500 mm^3 , all tumor-bearing mice were sacrificed to harvest tumor samples.

Statistical Analysis

Data were expressed as mean \pm SD and analyzed with GraphPad Prism 5.0 software. Data was analyzed by one-way analysis of variance (ANOVA) followed by LSD test. $p < 0.05$ was considered as statistically significant difference between groups.

Table 1. Growth Inhibition of Cultured Cells by Enoxacin.

Cell line	Origin	Enoxacin (IC ₅₀ , μM)	Taxol (IC ₅₀ , nM)
WPMY-1	Normal human prostate/stroma cell	>1000	>1000
A549	Lung adenocarcinoma	33.5 \pm 2.6	9.1 \pm 1.1
PANC-1	Pancreatic adenocarcinoma	160.3 \pm 14.3	15.3 \pm 1.4
HepG2	Hepatocellular carcinoma	183.2 \pm 13.9	29.2 \pm 3.8
PC-3	Prostate adenocarcinoma	20.2 \pm 2.3	19.5 \pm 2.2
DU145	Prostate carcinoma	21.5 \pm 2.5	13.8 \pm 1.5
LNCAp	Prostate carcinoma	25.3 \pm 3.6	18.7 \pm 1.7
C4-2	Prostate carcinoma	28.6 \pm 3.3	9.8 \pm 1.2
U251	Glioblastoma	135.6 \pm 12.8	19.1 \pm 1.8
SK-MES-1	Squamous cell carcinoma	88.7 \pm 8.3	7.5 \pm 0.6
MCF-7	Breast adenocarcinoma	176.6 \pm 16.1	26.1 \pm 2.3
MG-63	Osteosarcoma	115.3 \pm 11.2	16.5 \pm 1.7

Results

Enoxacin Inhibited the Proliferation of Prostate Cancer Cells

MTT assay was used to determine the anti-proliferative activities of Enoxacin on different cancer cells. Enoxacin had low toxicity to the normal human prostate/stroma cells, but selectively inhibited the proliferation of prostate cancer cells (Table 1). PC-3 cells have higher metastatic potential compared to other prostate carcinoma cells, such as DU145 or LNCAp cells. Moreover, IC₅₀ value of Enoxacin was lower on PC-3 cells (Table 1), indicating Enoxacin was more potent on PC-3 cells. Therefore, PC-3 cell line was chosen for the remaining experiments. Our results showed that Enoxacin

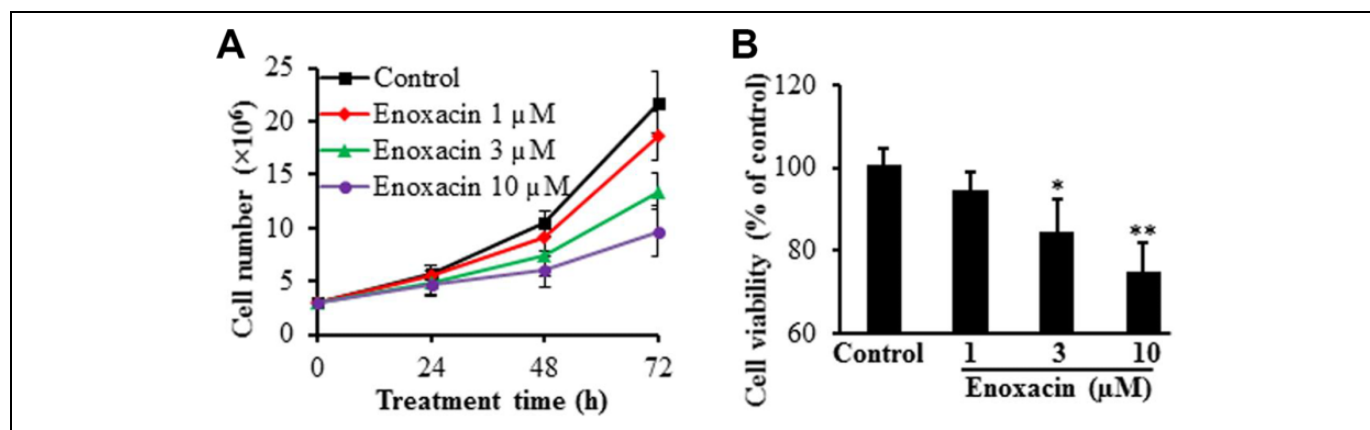


Figure 1. Enoxacin inhibited PC-3 cell proliferation. PC-3 cells were treated with Enoxacin at 1, 3, 10 μM up to 72 h. Cell number was counted (A) and cell viability was measured by MTT assay (B). Data were expressed as mean \pm SD (n = 3). * $p < 0.05$, ** $p < 0.01$ vs. control group.

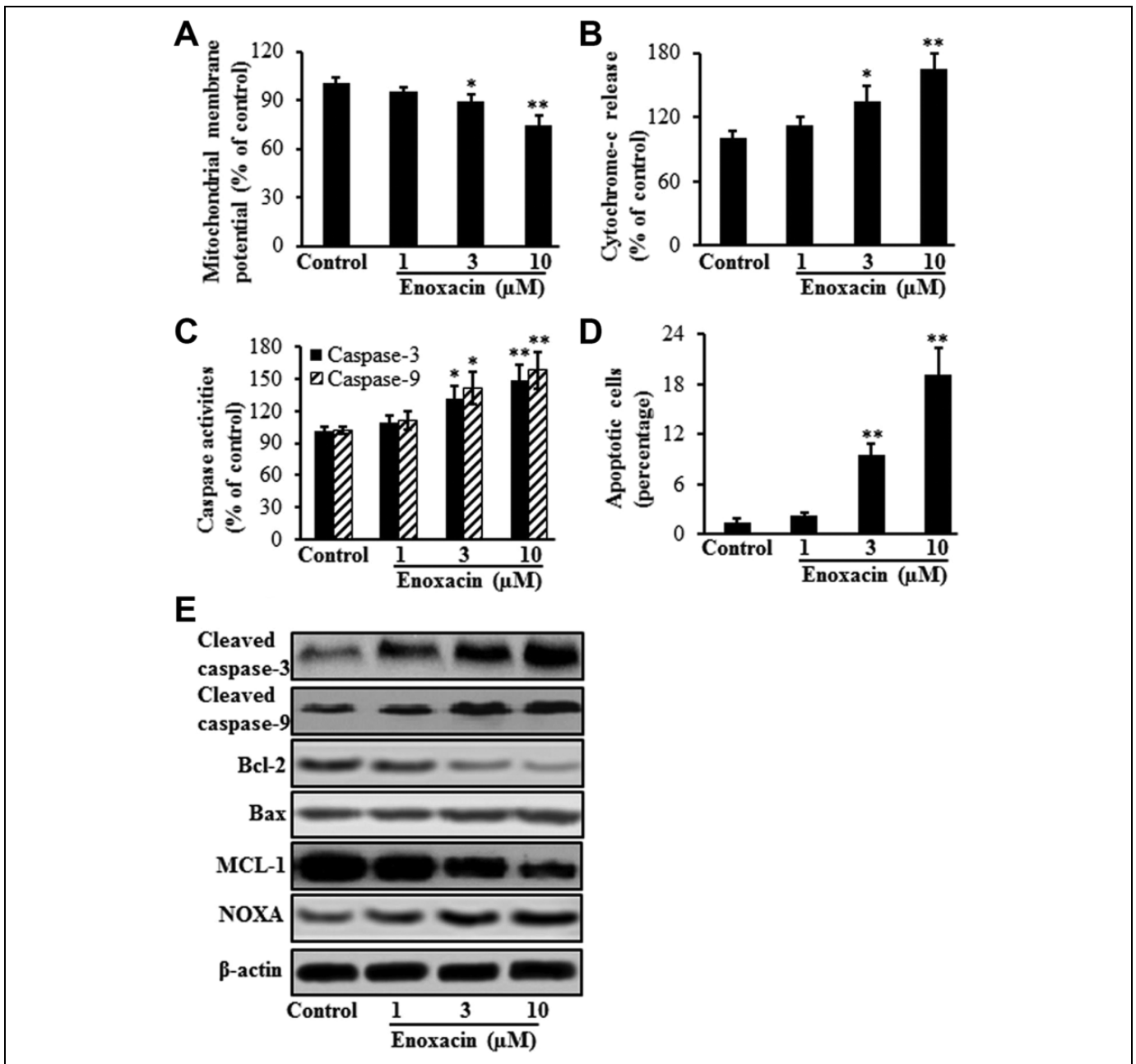


Figure 2. Enoxacin induced PC-3 cell apoptosis. After treatment for 48 h, Enoxacin caused depolarization of MMP (A); increased the release of cytochrome-c (B); increased caspase activities (C); and increased apoptosis detected by Annexin V/PI staining (D). Moreover, Enoxacin treatment changed apoptosis-related protein expression in PC-3 cells (E). Data were expressed as mean \pm SD (n = 3). * $p < 0.05$, ** $p < 0.01$ vs. control group.

demonstrated potent anti-proliferative activities against PC-3 cells in a dose-dependent manner, evidenced by counting the cell number and MTT assay (Figure 1).

Enoxacin Induced Apoptosis of PC-3 Cells

To investigate whether the decreased cell viability by Enoxacin involved apoptosis, the apoptosis-related markers were detected after Enoxacin treatment. Compared with the control group, Enoxacin treatment significantly decreased MMP;

increased cytochrome-c release and caspase-3/9 activities; and induced apoptosis in PC-3 cells. Pro-apoptotic protein Bax, cleaved caspase-3, cleaved caspase-9 and NOXA expression increased, but anti-apoptotic protein Bcl-2 and MCL-1 expression decreased after Enoxacin treatment (Figure 2).

Enoxacin Increased Autophagy of PC-3 Cells

Effects of Enoxacin on PC-3 cell autophagy were explored by examining the mRNA expression of *Beclin-1* and protein levels

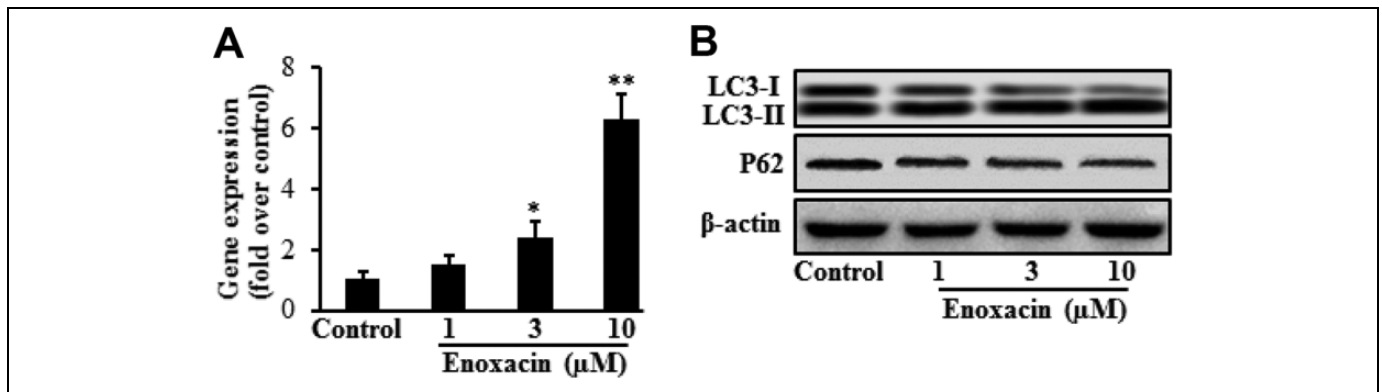


Figure 3. Enoxacin induced autophagy in PC-3 cells. PC-3 cells were treated with Enoxacin at 1, 3, 10 μM for 48 h. Cells were collected to measure the mRNA and protein expression: (A) *Beclin-1* mRNA expression; (B) LC3-I/LC3-II and P62 protein expression. Data were expressed as mean ± SD (n = 3). **p* < 0.05, ***p* < 0.01 vs. control group.

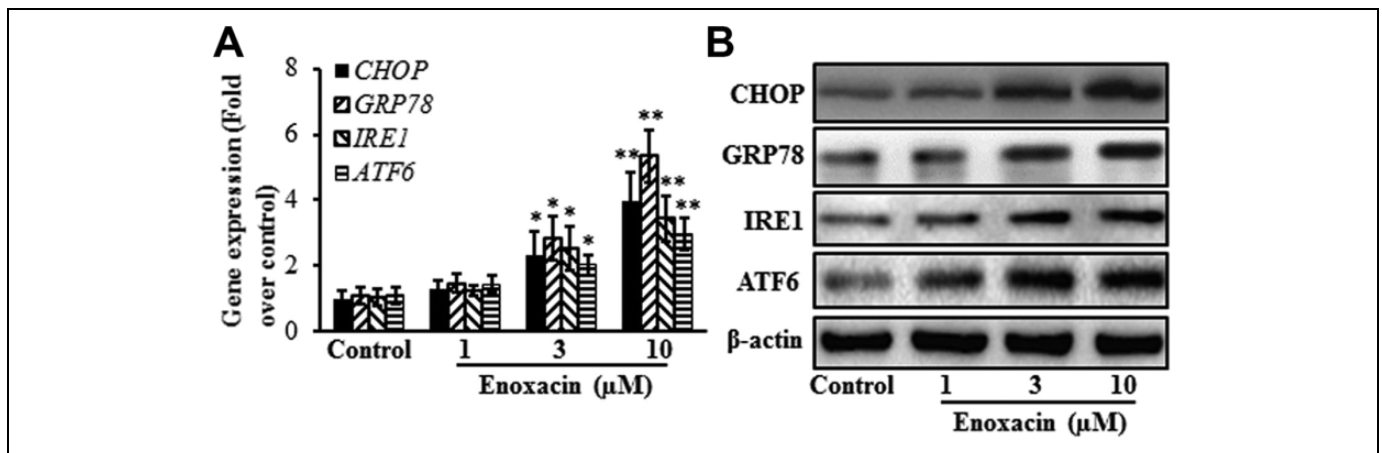


Figure 4. Enoxacin treatment triggered ER stress. After treatment for 48 h, Enoxacin increased the gene and protein expression of ER stress markers CHOP, GRP78, IRE1 and ATF6 (A, B). Data were expressed as mean ± SD (n = 3). **p* < 0.05, ***p* < 0.01 vs. control group.

of LC3-I/LC3-II as well as P62. Our results showed that Enoxacin significantly increased *Beclin-1* mRNA expression in a concentration-dependent manner. LC3-II protein expression slightly increased, whereas LC3-I protein expression was clearly reduced after Enoxacin treatment. Moreover, P62 protein expression also decreased after Enoxacin treatment (Figure 3). *These data suggested that Enoxacin treatment increased autophagy in PC-3 cells.*

Enoxacin Triggered ER Stress

Compared with the control group, Enoxacin treatment triggered ER stress, evidenced by the up-regulation of gene and protein expression of ER stress markers CHOP, GRP78, IRE1, and ATF6 (Figure 4).

Enoxacin Slowed Tumor Growth in Xenograft Mouse Model

Tumor-bearing mice were treated with Enoxacin at 1 or 2 mg/kg. Enoxacin treatment at 2 mg/kg significantly slowed tumor

growth, evidenced by both tumor volume and tumor weight. Moreover, Enoxacin treatment increased the DNA fragmentation showed by TUNEL assay (Figure 5).

Discussion

Although the survival of early-stage patients with prostate cancer has been improved significantly, the current treatment strategies remain unsatisfactory, largely due to the lack of effective therapeutic approaches.^{13,14} To search for new therapeutics, we reported a known compound Enoxacin, evaluated its anticancer activities and further elucidated the underlying mechanisms against prostate cancer, one most frequently encountered cancer in men.

Mammals have evolved complex death pathways, many of which converge on apoptotic programs via the mitochondria.¹⁵ During the process of apoptosis, internal death cues trigger the depolarization of mitochondrial membrane potential as a prerequisite to release the cytochrome-c from mitochondrial into the cytosol. Released cytochrome-c binds with the apoptotic protease activation factor to activate caspase-9.¹⁶ Activated

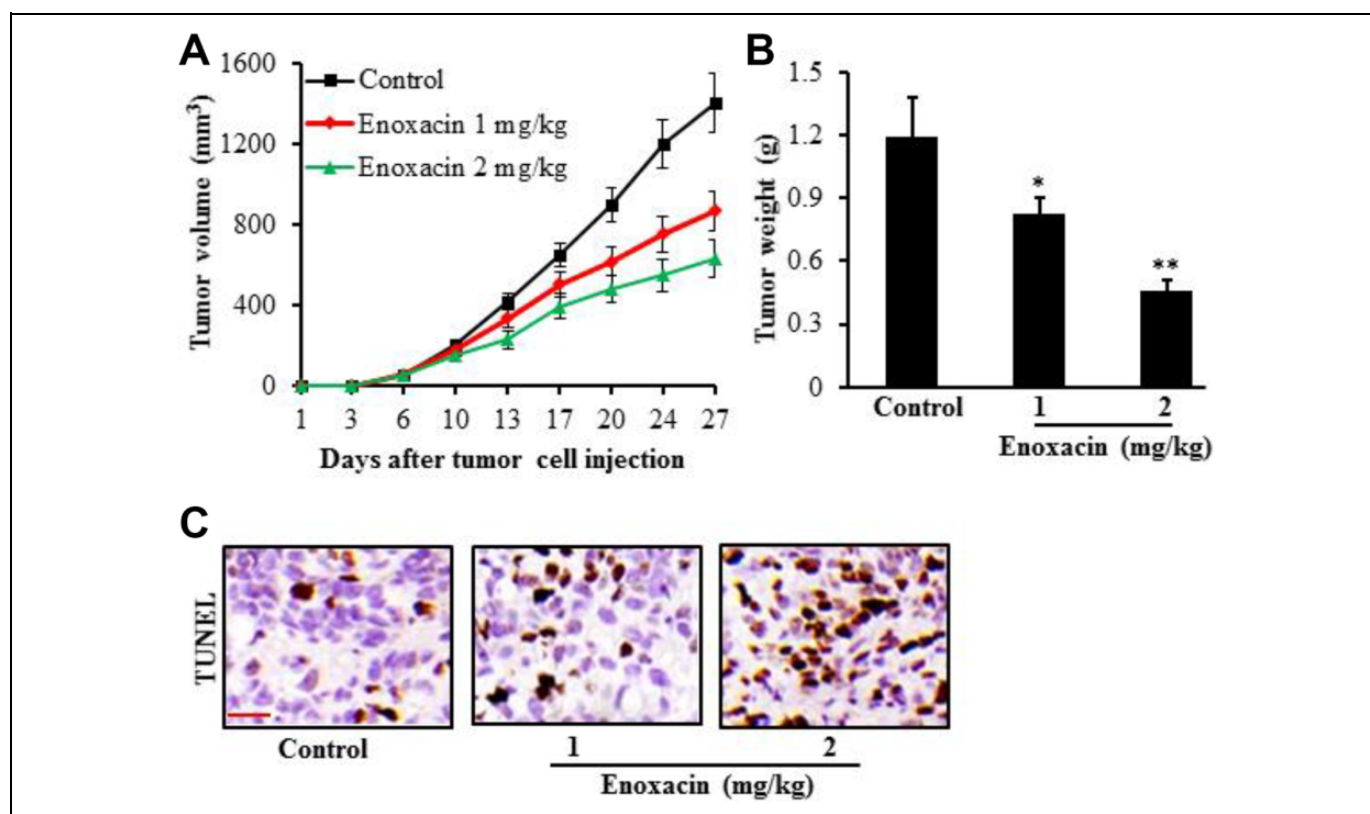


Figure 5. Enoxacin treatment slowed the human prostate tumor growth in nude mice. Enoxacin treatment decreased the tumor volume (A) and tumor weight (B); Enoxacin treatment increased the DNA fragmentation in tumors (magnification $\times 400$, scale bar = 25 μm) (C). Data were expressed as mean \pm SD (n = 5). * $p < 0.05$, ** $p < 0.01$ vs. control group.

caspase-9 together with the caspase-3, an apoptotic executor, activates endonucleases to cleave nuclear DNA and ultimately leads to cell death.¹⁷ Bcl-2 family play pivotal roles in the regulation of apoptosis in various cancers.¹⁸ As a crucial pro-apoptotic protein in the Bcl-2 family, NOXA could interact with the anti-apoptotic protein MCL-1 to trigger the apoptosis.^{19,20} NOXA/MCL-1 axis has been reported to be involved in apoptosis in many tumor models.²¹ Our results demonstrated that Enoxacin exerted the anti-cancer activities through inducing apoptosis mainly mediated by mitochondrial dysfunction, increased cytochrome-c release and activities of caspase-3/9. Anti-apoptotic protein expression decreased, but pro-apoptotic protein expression increased.

Autophagy plays an important role in cell metabolism, which can degrade intracellular macromolecules and damaged organelles to maintain cell homeostasis.²² Autophagy is associated with cell apoptosis as a form of programmed cell death.²³ Recent research shows that chemotherapeutic drugs could induce autophagy to increase apoptosis in cancer cells.²⁴ Our results showed that exposing PC-3 cells to Enoxacin caused autophagy, evidenced by a significant increase in the expression of *Beclin-1* gene, and decrease in the protein expression of LC3-I and P62.

Many mutations associated with cell damage result in the production of misfolded proteins.²⁵ If the misfolded proteins are not efficiently degraded, they accumulate in the ER to cause

ER stress and activate apoptotic program.²⁶ The ER stress elicits the secretion of misfolded proteins to induce unfolded protein response (UPR) signaling,^{27,28} which exerts a lot of essential functions via the protein-misfolding capability of ER stress-mediated cell apoptosis.²⁹ As a transcription factor, C/EBP homologous protein (CHOP) is an initiator of the ER stress-induced apoptotic process.²⁷ Furthermore, studies have established that the secretion of GRP78 is a marker for ER stress, due to its role as a major ER chaperone and its ability to control the activation of transmembrane ER stress sensors (IRE1 and ATF6).³⁰ As signaling proteins in ER stress, IRE1 stimulates activation of the apoptotic-signaling kinase-1, which activates downstream of stress kinases to promote apoptosis, and ATF6 translocates to the Golgi compartment where it is cleaved upon ER stress.³¹ Many chemotherapeutics activate ER response while inducing apoptosis in cancer cells.³² In this study, our data demonstrated that Enoxacin increased the gene and protein levels of CHOP, GRP78, IRE1 and ATF6, which are hallmarks of ER stress. ER stress is required in mitochondria-dependent apoptosis in PC-3 cells following Enoxacin treatment. Notably, this first-time finding might be a novel mechanism of Enoxacin-induced ER stress and apoptosis.

In conclusions, our study demonstrated that Enoxacin effectively induced apoptosis in PC-3 cells both *in vitro* and *in vivo*. Its underlying mechanism is most likely to be linked to the ER

stress, providing the scientific rationale to develop Enoxacin as a promising new therapeutic agent against prostate cancer.

Authors' Note

HYX conceived and designed the research. MHM and RZ performed experiments and statistical analysis. MHM and QZ drafted the manuscript. All authors read and approved the final manuscript. The animal procedures were approved by the Institutional Animal Care and Use Committee of the Fourth Affiliated Hospital of China Medical University with the animal experiment protocol No. (2018-1133) and performed in strict accordance with the regulation of the Use of Animals.


Declaration of Conflicting Interests

The author(s) declared no potential conflicts of interest with respect to the research, authorship, and/or publication of this article.

Funding

The author(s) received no financial support for the research, authorship, and/or publication of this article.

ORCID iD

Hongyan Xu, BS  <https://orcid.org/0000-0001-9899-9809>

References

- Torre LA, Siegel RL, Ward EM, Jemal A. Global cancer incidence and mortality rates and trends—an update. *Cancer Epidemiol Biomark Prev.* 2016;25(1): 16-27.
- Zhou Y, Bolton EC, Jones JO. Androgens and androgen receptor signaling in prostate tumorigenesis. *J Mol Endocrinol.* 2015; 54(1):15-29.
- Hammerer P, Manka L. Docetaxel or abiraterone in combination with androgen deprivation therapy for metastatic prostate cancer. *Urologe A.* 2019;58(10):1185-1197.
- Chen JR, Ni YC, Sun GX, et al. Comparison of current systemic combination therapies for metastatic hormone-sensitive prostate cancer and selection of candidates for optimal treatment: a systematic review and Bayesian network meta-analysis. *Front Oncol.* 2020;10:519388.
- Goldar S, Khaniani MS, Derakhshan SM, Baradaran B. Molecular mechanisms of apoptosis and roles in cancer development and treatment. *Asian Pac J Cancer Prev.* 2015;16(6):2129-2144.
- Zhao X, Kong F, Wang L, Zhang H. c-FLIP and the NOXA/Mcl-1 axis participate in the synergistic effect of pemetrexed plus cisplatin in human choroidal melanoma cells. *PLoS One.* 2017; 12(9):e0184135.
- Grzywa TM, Klicka K, Paskal W, et al. miR-410-3p is induced by vemurafenib via ER stress and contributes to resistance to BRAF inhibitor in melanoma. *PLoS One.* 2020;15(6):e0234707.
- Wang H, Yang Y, Chen H, et al. The predominant pathway of apoptosis in THP-1 macrophage-derived foam cells induced by 5-aminolevulinic acid-mediated sonodynamic therapy is the mitochondria-caspase pathway despite the participation of endoplasmic reticulum stress. *Cell Physiol Biochem.* 2014;33(6): 1789-1801.
- Chow SE, Kao CH, Liu YT, et al. Resveratrol induced ER expansion and ER caspase-mediated apoptosis in human nasopharyngeal carcinoma cells. *Apoptosis.* 2014;19(3):527-541.
- Cao SG, Sun R, Wang W, et al. RNA helicase DHX9 may be a therapeutic target in lung cancer and inhibited by enoxacin. *Am J Transl Res.* 2017;9(2):674-682.
- McDonnell AM, Pyles HM, Diaz-Cruz ES, Barton CE. Enoxacin and epigallocatechin gallate (EGCG) act synergistically to inhibit the growth of cervical cancer cells in culture. *Molecules.* 2019; 24(8):1580.
- Sousa E, Graca I, Baptista T, et al. Enoxacin inhibits growth of prostate cancer cells and effectively restores microRNA processing. *Epigenetics.* 2013;8(5):548-558.
- Komura K, Sweeney CJ, Inamoto T, Ibuki N, Azuma H, Kantoff PW. Current treatment strategies for advanced prostate cancer. *Int J Urol.* 2018;25(3):220-231.
- Wang JP, Xiao QY, Chen X, et al. LanCL1 protects prostate cancer cells from oxidative stress via suppression of JNK pathway. *Cell Death Dis.* 2018;9(2):197.
- Matt S, Hofmann TG. The DNA damage-induced cell death response: a roadmap to kill cancer cells. *Cell Mol Life Sci.* 2016;73(15):2829-2850.
- Zhang MZ, Zheng J, Nussinov R, Ma BY. Release of cytochrome C from Bax Pores at the mitochondrial membrane. *Sci Rep.* 2017; 7(1):2635.
- Liu H, Zhao M, Yang S, Gong DR, Chen DZ, Du DY. (2 R, 3 S)-pinobanksin-3-cinnamate improves cognition and reduces oxidative stress in rats with vascular dementia. *J Nat Med.* 2015;69(3): 358-365.
- Hetz CA. ER stress signaling and the BCL-2 family of proteins: from adaptation to irreversible cellular damage. *Antioxid Redox Signal.* 2007;9(12):2345-2355.
- Zhao X, Liu X, Su L. Parthenolide induces apoptosis via TNFRSF10B and PMAIP1 pathways in human lung cancer cells. *J Exp Clin Cancer Res.* 2014;33(1):3.
- Liu X, Lv Z, Zou J, et al. Afatinib down-regulates MCL-1 expression through the PERK-eIF2 α -ATF4 axis and leads to apoptosis in head and neck squamous cell carcinoma. *Am J Cancer Res.* 2016;6(8):1708-1719.
- Yan J, Zhong N, Liu G, et al. Usp9x- and Noxa-mediated Mcl-1 downregulation contributes to pemetrexed-induced apoptosis in human non-small-cell lung cancer cells. *Cell Death Dis.* 2014; 5(7):e1316.
- White E, Mehnert JM, Chan CS. Autophagy, metabolism and cancer. *Clin Cancer Res.* 2015;21(22):5037-5046.
- Kim MO, Lee HS, Chin YW, Moon DO, Ahn JS. Gartanin induces autophagy through JNK activation which extenuates caspase-dependent apoptosis. *Oncol Rep.* 2015;34(1):139-146.
- Shi SM, Tan P, Yan BD, et al. ER stress and autophagy are involved in the apoptosis induced by cisplatin in human lung cancer cells. *Oncol Rep.* 2016;35(5):2606-2614.
- Hetz C, Saxena S. ER stress and the unfolded protein response in neurodegeneration. *Nat Rev Neurol.* 2017;13(8):477-491.
- Duricka DL, Brown RL, Varnum MD. Defective trafficking of cone photoreceptor CNG channels induces the unfolded protein

- response and ER stress-associated cell death. *Biochem J.* 2012; 441(2):685-696.
27. Lu CC, Yang JS, Chiang JH, et al. Cell death caused by quinazolinone HMJ-38 challenge in oral carcinoma CAL 27 cells: dissections of endoplasmic reticulum stress, mitochondrial dysfunction and tumor xenografts. *Biochim Biophys Acta.* 2014;1840(7): 2310-2320.
28. Cheng X, Feng H, Wu H, et al. Targeting autophagy enhances apatinib-induced apoptosis via endoplasmic reticulum stress for human colorectal cancer. *Cancer Lett.* 2018; 431:105-114.
29. Kim C, Kim B. Anti-cancer natural products and their bioactive compounds inducing ER stress-mediated apoptosis: a review. *Nutrients.* 2018;10(8):1021.
30. Lee AS. The ER chaperone and signaling regulator GRP78/BiP as a monitor of endoplasmic reticulum stress. *Methods.* 2005;35(4): 373-381.
31. Sano R, Reed JC. ER stress-induced cell death mechanisms. *Biochim Biophys Acta.* 2013;1833(12):3460-3470.
32. Qin L, Wang Z, Tao L, Wang Y. ER stress negatively regulates AKT/TSC/mTOR pathway to enhance autophagy. *Autophagy.* 2010;6(2):239-247.